ACS APPLIED MATERIALS & INTERFACES

RESEARCH ARTICLE

www.acsami.org

Facile Preparation of Robust Microcapsules by Manipulating Metal-Coordination Interaction between Biomineral Layer and Bioadhesive Layer

Lei Zhang,[†] Jiafu Shi,[†] Zhongyi Jiang,[*,†,‡] Yanjun Jiang,[§] Ruijie Meng,[†] Yuanyuan Zhu,[†] Yanpeng Liang,[†] and Yang Zheng[†]

[†]Key Laboratory for Green Technology of Ministry of Education, School of Chemical Engineering and Technology, Tianjin University, Tianjin 300072, China

[‡]National Key Laboratory of Biochemical Engineering, Institute of Process Engineering, Chinese Academy of Sciences, Beijing 100190, China

[§]Department of Bioengineering, School of Chemical Engineering, Hebei University of Technology, Tianjin 300130, China

Supporting Information

ABSTRACT: A novel approach combining biomimetic mineralization and bioadhesion is proposed to prepare robust and versatile organic−inorganic hybrid microcapsules. More specifically, these microcapsules are fabricated by sequential deposition of inorganic layer and organic layer on the surface of $CaCO_3$ microparticles, followed by the dissolution of $CaCO_3$ microparticles using EDTA. During the preparation process, protamine induces the hydrolysis and condensation of titania or silica precursor to form the inorganic layer or the biomineral layer. The organic layer or bioadhesive layer was formed through the rapid, spontaneous oxidative polymerization of dopamine into polydopamine (PDA) on the surface of the biomineral layer. There exist multiple interactions between the inorganic layer and the organic layer. Thus, the as-prepared organic−inorganic hybrid microcapsules acquire much higher mechanical stability and surface reactivity than pure titania or pure silica microcapsules. Furthermore, protamine/titania/polydopamine hybrid microcapsules display superior mechanical stability to protamine/silica/polydopamine hybrid microcapsules because of the formation of Ti(IV)−catechol coordination complex between the biomineral layer and the bioadhesive layer. As an example of application, three enzymes are respectively immobilized through physical encapsulation in the lumen, in situ entrapment within the wall and chemical attachment on the out surface of the hybrid microcapsules. The as-constructed multienzyme system displays higher catalytic activity and operational stability. Hopefully, the approach developed in this study will evolve as a generic platform for facile and controllable preparation of organic−inorganic hybrid materials with different compositions and shapes for a variety of applications in catalysis, sensor, drug/gene delivery.

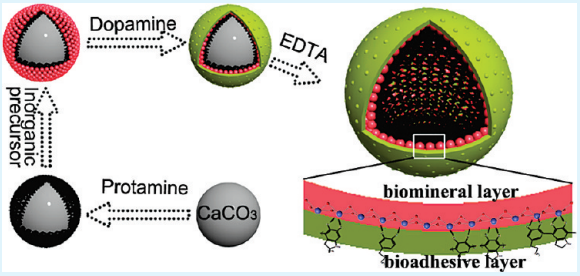

KEYWORDS: organic−inorganic hybrid microcapsules, biomineral layer, bioadhesive layer, metal-coordination interaction, mechanical stability

1. INTRODUCTION

Organic−inorganic hybrid microcapsules have displayed fascinating application potential in biomacromolecules encapsulation for catalysis, drug or gene delivery, biosensors, etc.[1−6] In nature, organic−inorganic hybrid materials are often produced by biomineralization process using biomacromolecules as both templates and catalysts to induce and control the formation and growth of the inorganic phase at ambient pressure and temperature, and neutral pH value. Through the intimate and multiple interactions between the organic and inorganic phases, these biominerals acquire their intricate structural characteristics and unique physicochemical and mechanical properties.[7−9] Therefore, biomineralization and biomimetic mineralization have been evolved as tools for the facile and green synthesis of hybrid materials with hierarchical organizations.[10−13] In our previous studies, organic−inorganic hybrid microcapsules have been prepared via biomimetic mineralization using protamine to induce the formation of silica and titania nanoparticles from water-soluble precursors.[14,15] Because the formation of titania and silica relies on the generation of covalent bonds, rather than on ionic interactions, titania and silica nanoparticles are both of amorphous feature. Accordingly, the mechanical strength of the resultant microcapsules is usually rather weak. Layer-by-layer self-assembly strategy has been employed to increase the mechanical

Received: December 3, 2010
Accepted: January 24, 2011
Published: February 4, 2011

stability of the microcapsules through noncovalent interactions, however, the assembly process has to be repeated many times to meet the mechanical requirements, and interlayer penetration/entanglement may also increase the difficulty in structure control.[16,17] Additionally, the chemical inertness of the microcapsule surface is disadvantageous for secondary treatment.

Fortunately, the above two problems, that is, mechanic stability and surface reactivity could be solved by the inspiration of exceptional bioadhesion system in nature. It is well-known that mussels anchor to surfaces in turbulent aqueous environments by injecting cuticular protein solution rich in the catecholic amino acid 3,4-dihydroxyphenyl-L-alanine (dopa) and inorganic ions, notably, Fe^{3+} onto the substrate surface and into a groove along the length of the foot.[18,19] The protein undertakes oxidative self-polymerization at near-neutral pH, ambient temperature within a short period. The mussel then repeats this process many times to ensure its strong attachment to the substrate.[20] Quite recently, iron has been found to bind these DOPA proteins for two separate, but closely related, purposes: to improve the mechanical performance of the threads and to enable the formation of the adhesive plaques.[21−23] It could be derived that cuticle is a polymeric scaffold stabilized by iron-catecholato coordination complexes. Inspired by mussel bioadhesion, Messersmith reported a simple but versatile surface modification approach to construct an active polydopamine (PDA) coating on a wide variety of materials.[24] Dopamine, as a kind of catecholamine, spontaneously polymerizes in solution under weak alkaline condition, the resultant PDA can readily and firmly attach the target surfaces.[25] After drying, the coated surfaces provide a reactive platform for secondary treatments, and produce a variety of functional materials to serve for different purposes.[26,27] Additionally, dopamine is also a bidentate chelating agent that has a particular affinity toward some metal ions that exhibit high oxidation states or high charge to metal ion radius ratios.[28,29]

Herein, a novel approach to prepare robust and versatile organic−inorganic hybrid microcapsules is proposed, utilizing two platform technologies: biomineralization and bioadhesion, as well as manipulating the coordination interaction between inorganic layer and organic layer. More specifically, the hybrid microcapsules are fabricated by sequential deposition of titania layer and polydopamine layer on the surface of $CaCO_3$ microparticles, followed by dissolution of the $CaCO_3$ microparticles using EDTA. The titania layer (biomineral layer) was formed through the hydrolysis and condensation of titanium bis(ammonium lactato)-dihydroxide (Ti-BALDH) induced by protamine, the polydopamine layer (bioadhesive layer) was formed through the spontaneous polymerization of dopamine. The strong coordination interaction between the biomineral layer and the bioadhesive layer rendered the microcapsules superior mechanical stability. The active groups such as quaternary ammonium groups and carboxyl groups on polydopamine endowed abundant reaction sites on the hybrid microcapsule surfaces. As comparison, protamine/silica/polydopamine (PSi-PDA) microcapsules were prepared following the similar protocol. The morphology, structure, and chemical composition of the hybrid microcapsules were characterized, and the relevant mechanism was tentatively discussed. To explore the application potential of the hybrid microcapsules, a multienzyme system containing three enzymes (α-amylase, β-amylase, and glucosidase) was constructed for converting starch to isomaltooligosaccharide (IMOs).

2. MATERIALS AND METHODS

α-glucosidase from *Aspergillus niger* (E.C.3.2.1.20, 85 wt % aqueous solution, 116 kDa) was purchased from Amano enzyme Inc., Japan. α-amylase (E.C.3.2.1.1, 47 kDa) and β-amylase (E.C.3.2.1.2, 57 kDa) were purchased from Kebaiao Biotechnology Co, China. Dopamine was purchased from Yuancheng Technology Development Co.Ltd. (Wuhan, China). Ti-BALDH (50 wt % aqueous solution), protamine sulfate from salmon, Poly(sodium 4-styrenesulfonate) (PSS, MW ∼70 000) and fluorescein isothiocyanate (FITC) was purchased from Sigma−Aldrich Chemical Co. Sodium silicate (Na_2SiO_4), tris(hydroxymethyl)amiomethane (Tris), hydrochloric acid (HCl), and ethylenediaminetetraacetic acid (EDTA) of reagent grade quality were obtained from Guangfu (Tianjin, China). The FITC-labeled enzyme was prepared as previously reported in the literature.[30]

In the synthesis of PTi-DPA microcapsules, PSS-doped $CaCO_3$ microparticles were used as sacrificial templates, which were prepared according to the coprecipitation method previously described in the literature.[31] Briefly, PSS (60 mg) was completely dissolved in 20 mL of $CaCl_2$ solution (0.33 M) in a beaker at room temperature. Then, an equal volume of Na_2CO_3 solution (0.33 M) was rapidly added into the beaker under magnetic agitation, and stirred continuously for 20 s. After setting for 10−15 min, the precipitate was centrifuged, and washed three times with water. Finally, PSS-doped $CaCO_3$ microparticles with spherical shape about 3 μm in size were obtained.

In a typical preparation of PTi-DPA microcapsules, the PSS-doped $CaCO_3$ microparticles were first dispersed in protamine aqueous solution (5 mL, 2 g/L) containing NaCl (0.5 M). After shaking for 15 min, $CaCO_3$ microparticles coated with protamine were collected by centrifugation and washed twice with water to remove the residual protamine. Subsequently, these microparticles were suspended in Ti-BALDH solution (5 mL, 1.25 wt %), and shaken for 15 min. After centrifuged and washed twice with water, $CaCO_3$ microparticles coated with protamine layer and titania layer were obtained. The resultant microparticles was combined and resuspended in 20 mL of Tris-HCl buffer (0.1M, pH 8.5) with a concentration of 2 g/L of dopamine hydrochloride, and the suspension was allowed to proceed for 8 h with constant shaking. Next, the tan colored particles were centrifuged (3000 g, 2 min) and washed with fresh Tris-HCl buffer until the supernatant became colorless. PTi-DPA microcapsules were obtained after removal of $CaCO_3$ cores through incubating the microparticles in EDTA solution (0.05 M). Protamine/titania (PTi) microcapsules were prepared in a similar procedure in the absence of dopamine.

In a typical preparation of protamine/silica/polydopamine (PSi-DPA) microcapsules, similarly, the prepared PSS-doped $CaCO_3$ microparticles was coated protamine(2 g/L), Na_2SiO_4(30 mM, pH 8.0) and dopamine(2 g/L, pH8.5 Tris-HCl) successively, followed by dissolution of $CaCO_3$ cores using EDTA(0.05M). Protamine/silica (PSi) microcapsules were prepared in a similar procedure in the absence of dopamine.

The morphology of the microcapsules was observed by SEM (Philips XL30 ESEM). The microchemical analysis and element mapping were conducted by EDS (Oxford) attached to the SEM. The cross-section morphology of the microcapsule was observed by an FESEM (Hitachi S-4800, Japan) instrument. All specimens were gold-sputtered to prevent charging. TEM observation was performed on a JEM-100CX instrument, and the crystallinity of the nanocomposites was measured by SAED attached to the TEM. FTIR spectra of the nanocomposites and the microcapsule shell were obtained using a Nicolet-560 spectrometer. A total of 32 scans were accumulated with a resolution of 4 cm^{-1} for each spectrum. The elemental composition of the microcapsule surface was analyzed by XPS in a Perkin-Elmer PHI 1600 ESCA system with a monochromatic Mg Kα source and a charge neutralizer. A solution of FITC-labeled microcapsules was mixed with an equal amount of PSS solution of different concentrations and incubated for 10 h. More than

200 microcapsules were inspected at each PSS concentration. The deformation ratio was defined as the number of deformed microcapsules divided by the total number of microcapsules. Fluorescence microscope images were taken using an Olympus BX51 microscope with a × 100 oil immersion objective lens (Olympus, Tokyo, Japan). Fluorescence microscope images were employed to determine the number of invaginated microcapsules. UV−visible spectra were acquired using a UV spectrophotometer (Hitachi U-2800).

To immobilize three enzymes by the PTi-DPA (PSi-DPA) microcapsule, 1 mL of glucosidase was added during the coprecipitation process to prepare the PSS-doped $CaCO_3$ microparticles. As sacrificial templates, glucosidase-containing $CaCO_3$ microparticles were first dispersed in protamine aqueous solution (5 mL, 2 g/L) containing NaCl (0.5 M),[32] shaken for 15 min, collected by centrifugation, and washed twice with water to remove the residual protamine. Subsequently, these microparticles were suspended in 5 mL of 1.25 wt % Ti-BALDH solution (or 30 mM Na_2SiO_4 solution) and shaken for 15 min. After they were centrifuged and washed twice with water, the microparticles were resuspended in Tris-HCl (0.1 M pH 8.5) solution containing β-amylase and dopamine for 8 h with constant shaking. Next, the tan particles were centrifuged (3000 g, 2 min) and washed three times with fresh Tris-HCl buffer. Finally, the resultant microparticles were resuspended in α-amylase solution for 8 h with constant shaking at room temperature. The decomposition of the $CaCO_3$ microparticles by EDTA treatment was performed as previously described, and the enzyme-containing microcapsules was immersed into 0.15 M $CaCl_2$ for 15 min to reactivate enzyme molecules (α-amylase is calcium-dependent enzyme, and the activity was recovered by immersing in $CaCl_2$ aqueous solution.).

Enzyme activity: The activities of free and immobilized multienzyme were evaluated by the consecutive bioconversion of starch and calculated based on the amounts of isomaltooligosaccharide (IMOs) produced. The IMOs concentration was determined by HPLC as described in our previous study.[33]

Immobilization yield: The enzyme immobilization yield was determined by eq 1.

$$\text{immobilization yield}(\%) = \frac{U_{\text{immobilized}}}{U_{\text{initial}}} \times 100 \quad (1)$$

Where $U_{\text{immobilized}}$ and U_{initial} are the activities of immobilized enzyme and free enzyme in the original solution, respectively.

Recycling stability of immobilized enzyme: The recycling stability of immobilized enzyme was determined by eq 2.

$$\text{recycling efficiency}(\%) = \frac{\text{enzyme activity in the } n\text{th cycle}}{\text{enzyme activity in the 1st cycle}} \times 100\% \quad (2)$$

3. RESULTS AND DISCUSSION

Scheme 1 illustrates the major steps involved in the preparation of PTi-PDA microcapsules. Spherical-shaped $CaCO_3$ microparticles with ~3 μm diameter obtained by a common coprecipitation technique were used as sacrificial templates for the preparation of PTi-PDA microcapsules. To ensure the homogeneous distribution of $CaCO_3$ microparticles and endowed the surface of $CaCO_3$ microparticles with negative charge, PSS was added to $CaCO_3$ microparticle during the coprecipitation process.[34] Figure S1 shows typical scanning electron microscopy (SEM) images of $CaCO_3$ microparticles prepared by coprecipitation method. It can be seen that $CaCO_3$ microparticles exhibited well-defined spherical shape about 3 μm in diameter. Therefore, the $CaCO_3$ microparticles were negatively charged when immersed into the positively charged protamine

Scheme 1. Schematic Representation of the Formation Process of the PTi-PDA(PSi-PDA) Microcapsule

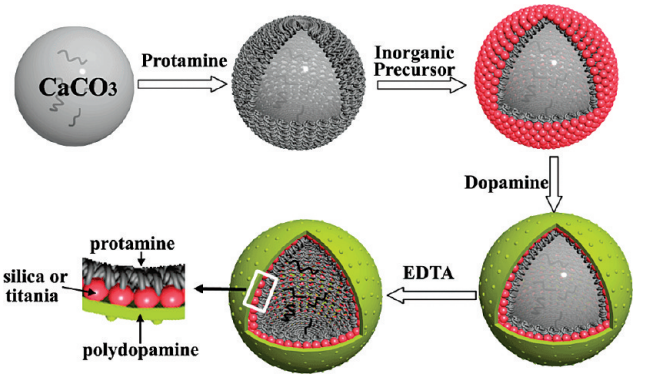

solution at pH 7.0. The guanidyl groups of protamine were prone to be attracted by $CaCO_3$ microparticles through electrostatic attractive interaction, thus triggering a facile deposition of protamine on the $CaCO_3$ microparticles surface and rendering a positively charged layer. When these freshly formed $CaCO_3$/protamine microparticles were kept in contact with the Ti-BALDH solution, the free cationic guanidyl groups of protamine enriched the Ti-BALDH in the solution via electrostatic attraction, leading to an increased Ti-BALDH concentration around the protamine molecules, enabling the biomimetic titanification process. A titania outer shell was thus formed as the Ti-BALDH condensation accomplished.[14] Next, negatively charged $CaCO_3$/protamine/titania microparticles were resuspended in 0.1M, pH 8.5 Tris-HCl buffer with dopamine hydrochloride. Instantly, a yellow colored suspension for $CaCO_3$/protamine/titania was formed and gradually changed into tan color. Since dopamine has a high affinity toward transition metal ions, and titanium ions can bind either two or three dopamine molecules to form bis- and tris-complexes, the yellow color should be ascribed to the dopamine-to-titania charge-transfer complex, and the tan color should be ascribed to the self-polymerization of dopamine.[28] Although the exact polymerization mechanism of dopamine remains elusive at present, it was incrementally accepted that the catechol groups were first oxidized into the quinones which further participated in intramolecular cyclization and a variety of intermolecules cross-linking reactions, including aryl−aryl coupling, Michael-type addition reaction, and Schiff base substitution. After the spontaneous self-polymerization of dopamine on the surface of $CaCO_3$/protamine/titania microparticles, and the subsequent dissolution of $CaCO_3$ using EDTA, the robust PTi-PDA microcapsules were finally acquired. For comparison, protamine/titania (PTi), protamine/silica (PSi) and PDA microcapsules[16,17] and protamine/silica/polydopamine(PSi-PDA) microcapsule were prepared at the same time.

The morphology and size of the resultant microcapsules were observed by SEM and TEM. Figures 1a, S2a, and S2c showed the SEM images of PTi-PDA microcapsules, PTi microcapsules and PDA microcapsules, respectively. Both PTi and PDA microcapsules collapsed after drying and exhibited the morphology of folds and creases, suggesting the low mechanical strength. In contrast, PTi-PDA microcapsules kept a regular spherical shape, and their diameters were around 3−4 μm. The TEM verified the hollow structure of PTi-PDA microcapsules and the SAED analysis confirmed the amorphous nature of the titania precipitates (Figure 1b). High contents of carbon and oxygen, the

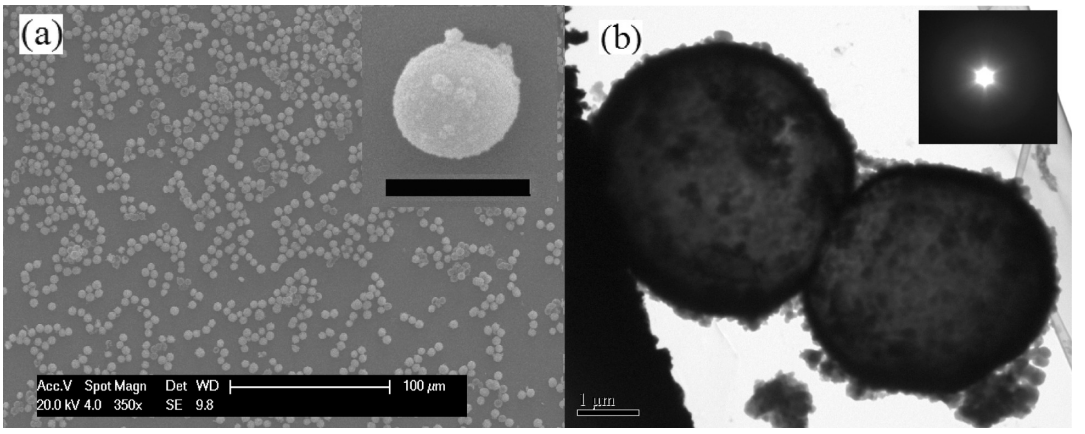

Figure 1. (a) SEM photographs of PTi-PDA microcapsules (inset scale bar 5 μm). (b) TEM photograph of PTi-PDA microcapsules (inset was the SAED pattern).

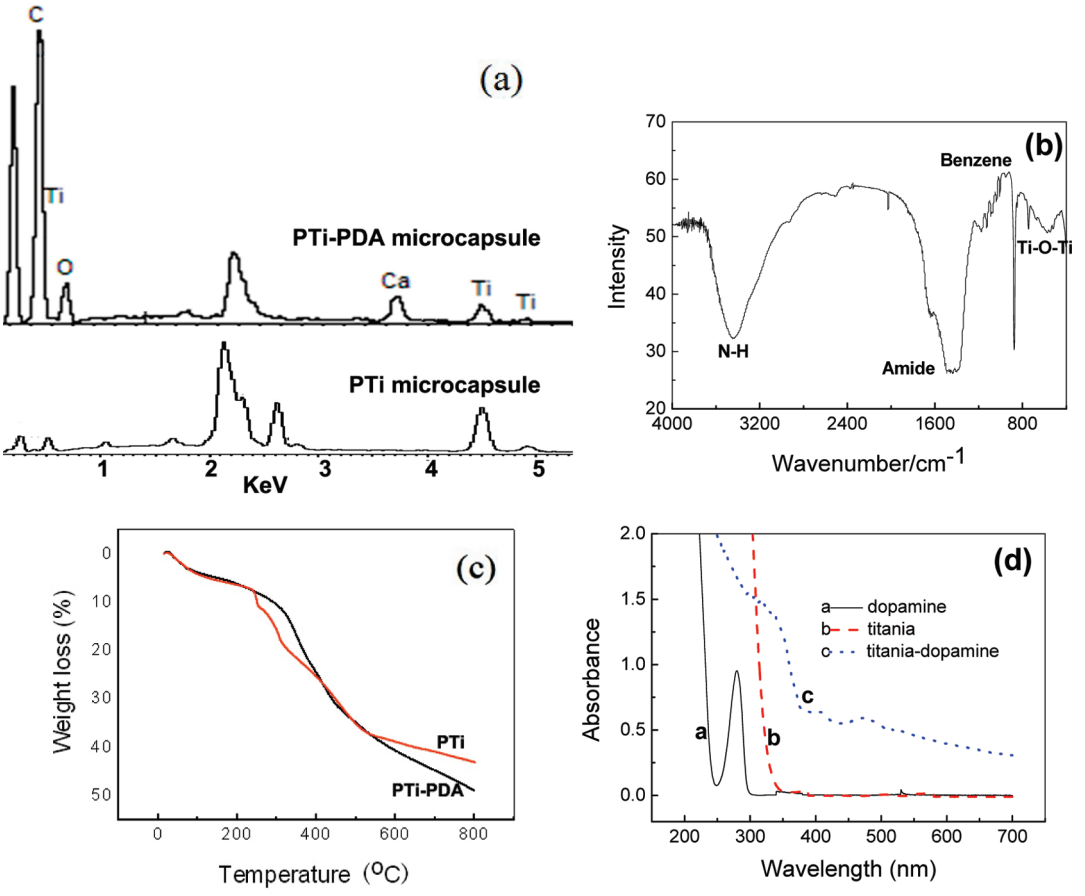

Figure 2. (a) EDS of the PTi and PTi-PDA microcapsules. (b) FTIR of the PTi-PDA microcapsules. (c) TGA of the PTi and PTi-DPA microcapsules. (d) UV−visible spectra for dopamine, titania and titania-dopamine complex in water.

composition of dopamine, were detected on the PTi-PDA microcapsules surface, and titanium in the subsurface was also detected by EDS (Figure 2a). As shown in Figure 2b, the FTIR spectra of PTi-PDA microcapsules had a broad absorption near 3400 cm^{-1}, which were characteristic of primary amines. The broad band at around 450−700 cm^{-1} could be attributed to the absorption of Ti−O−Ti, which indicated the formation of titania. The absorption bands in 900−1300 cm^{-1} from benzene ring and phenol hinted the existence of dopamine. Evidence for the composition of organic and inorganic material in the hybrid microcapsule was also probed by thermogravimetric analysis (TGA). As shown in Figure 2c, the ∼10% weight loss up to 300 °C was attributed to the physically adsorbed water and bound water and, ∼ 23% weight loss was due to the decomposition of protamine and polydopamine. As shown in Figure 2d, the formation of titania-catechol coordination complex was confirmed by UV−visible spectra. In addition to the absorption of titania in the wavelength less than 360 nm, the titania-catechol

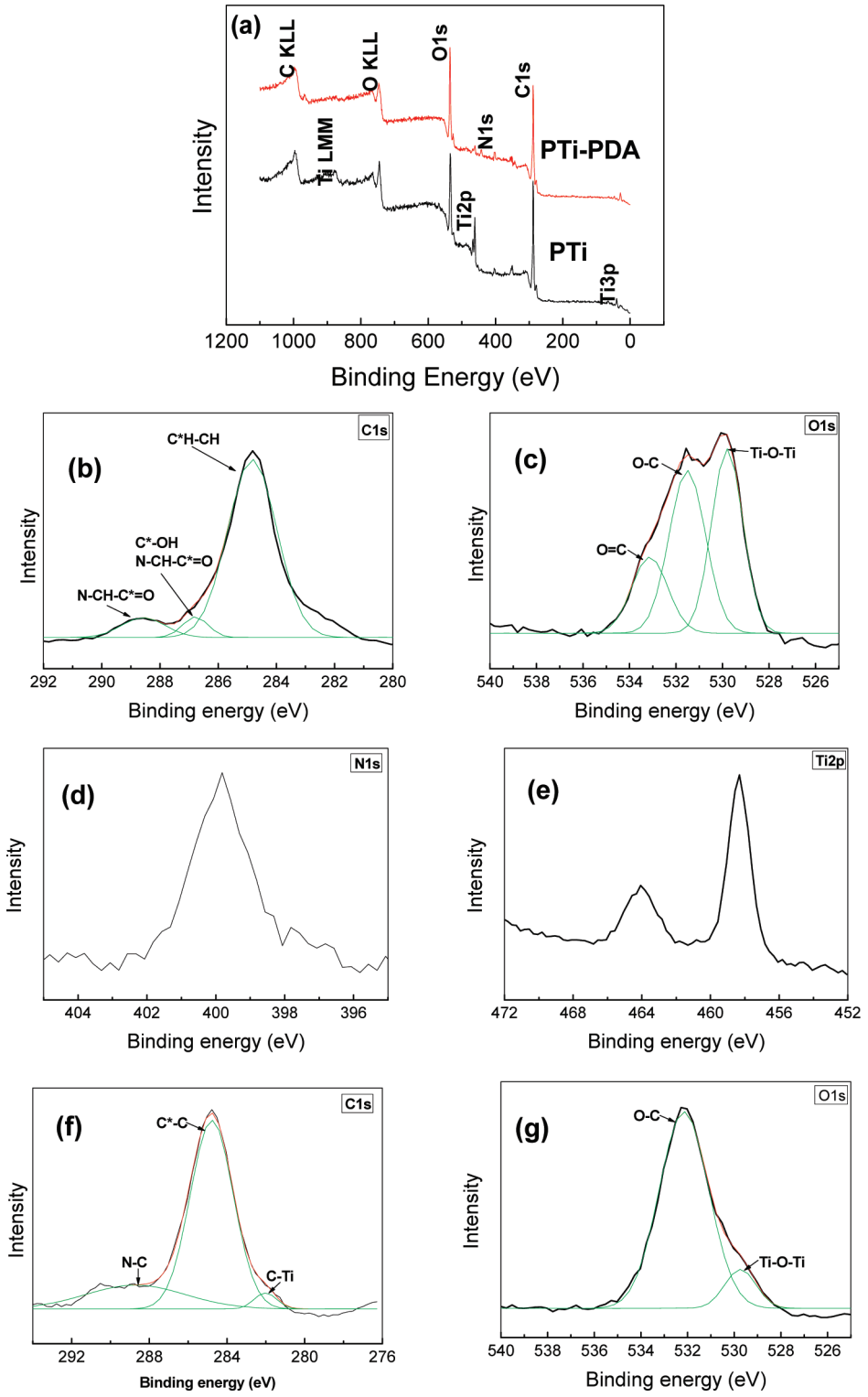

Figure 3. (a) XPS of the PTi-PDA and PTi microcapsules. High- resolution spectra of C1s (b), O1s (c), N1s (d), and Ti2p (e) of PTi microcapsules. High-resolution spectra of C1s (f) and O1s (g) of PTi-PDA microcapsules.

coordination complex showed a new broad absorption band spanning the whole visible range.[35,36] X-ray photoelectron spectroscopy (XPS) was conducted to probe the surface element composition of PTi-PDA and PTi microcapsules. As shown in Figure 3a, there were C, O, Ti, and N elements in XPS survey spectrum of PTi microcapsules. The C, N, and some O elements should originate from protamine sulfate occluded in microcapsules. The Ti and some O elements may originate from titania. Figure 3b−e showed the high-resolution XPS spectra of C1s, N1s, O1s, and Ti2p regions, respectively. It was found that the C1s XPS spectrum was composed of three peaks at 284.8, 286.4, and 288.3 eV. They could be assigned to aliphatic C*H−CH

which was originated from protamine, oxidrilic C*−OH, and amidic N−C*H−CO and N−CH−C*−O in the amidic group, where the respective carbon species were marked by asterisk, respectively.[37] One peak of N1s at 400.2 eV was originated from protamine. High-resolution XPS spectrum of O1s exhibited three peaks at 529.8, 532, and 533.2 eV, which could be assigned to Ti−O−Ti, C−O, and C═O bond, respectively. In the high-resolution XPS spectrum of Ti2p, the binding energies of $Ti2p_{3/2}$ and $Ti2p_{1/2}$ were centered at 458.8 and 464.6 eV, respectively. This clearly revealed that the titanium elements were in the oxidation state IV, corresponding to Ti^{4+} (TiO_2).[14] Compared with PTi-PDA microcapsules, there were C, O, N and trace amounts of Ti elements in XPS survey spectrum. And Figure 3f-g showed the high-resolution XPS spectra of C1s and O1s region, respectively. It was found that the C1s XPS spectrum was composed of three peaks at 282.0, 284.8 and 288.3 eV- (Figure 3f). These peaks could be assigned to aliphatic C*−C and oxidrilic C*−N, which was originated from dopamine, and amidic C*−Ti was formed during the complexation process of colloidal titanium dioxide by dopamine. High-resolution XPS spectrum of O1s exhibited two peaks at 529.8 and 532 eV (Figure 3g), which could be assigned to Ti−O−Ti and C−O bond. The characterization of PSi-PDA microcapsule was described in the Supporting Information.

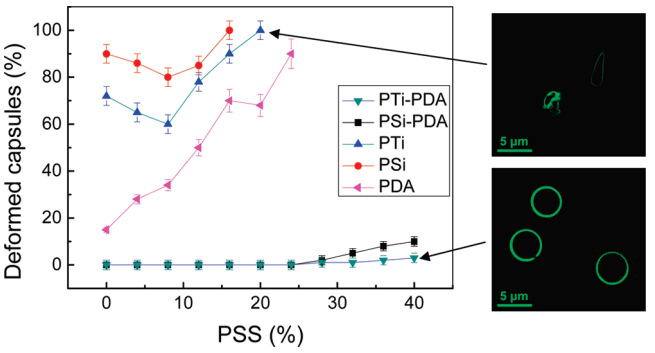

Figure 4. Percentage of deformed microcapsules as a function of the PSS concentration. The figures on the right side were the typical microscopy image of intact and deformed microcapsule.

The mechanical stability of microcapsules was investigated by the method of penetrated pressure in different concentration of PSS aqueous solution. Briefly, microcapsules kept their initial shape at low PSS concentration, and microcapsules broke or shrunk at a very high PSS concentration. Unlike water molecule, PSS molecule was very large (MW ca.70.000), which could not pass through the microcapsule wall. The shrinking/buckling of

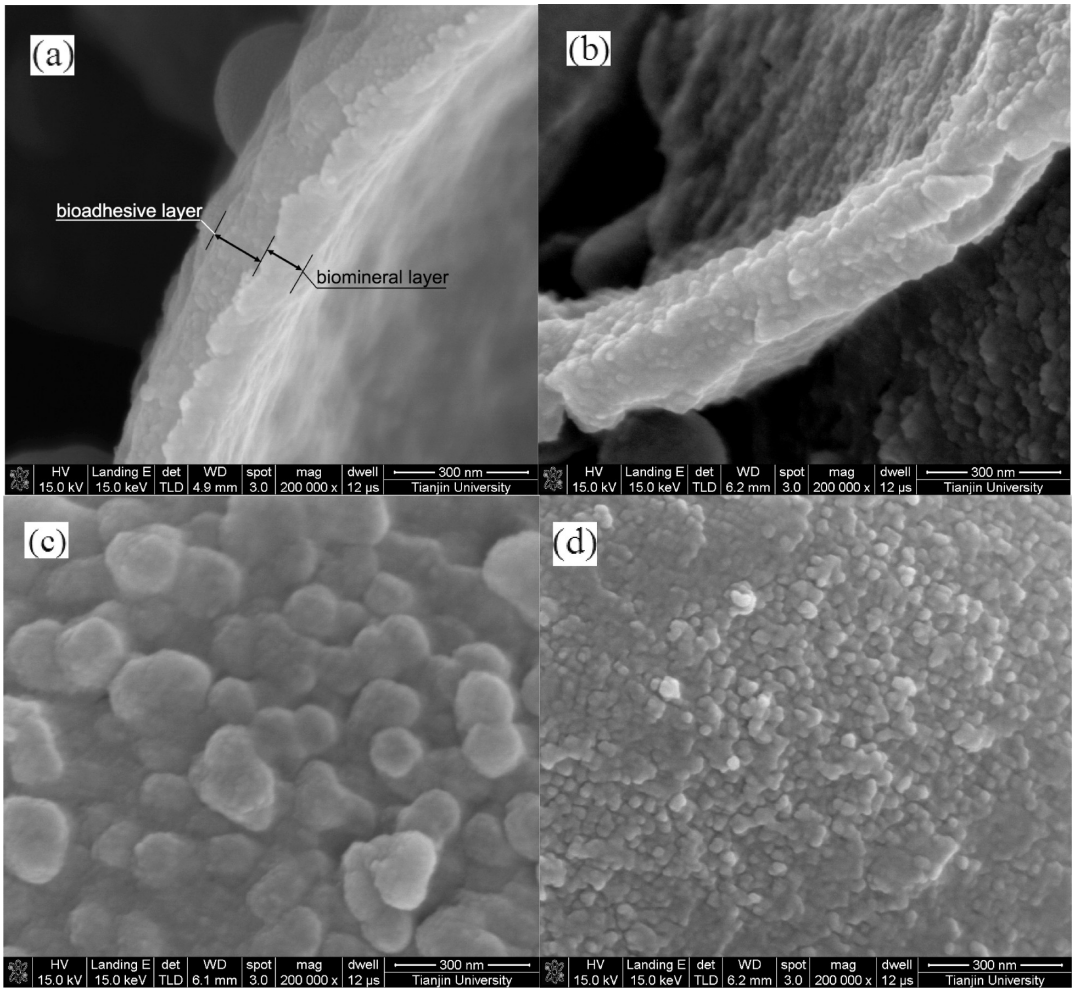

Figure 5. (a) Cross section of the PTi-PDA microcapsules, (b) cross section of the PSi-PDA microcapsules, (c) the surface of the PTi-PDA microcapsules, and (d) the surface of the PSi-PDA microcapsules.

Table 1. Immobilization Efficiencies for Enzymes in Different Microcapsules

	immobilization efficiency (%)			
enzyme	PTi-PDA	PTi	PSi-PDA	PSi
α-amylase	46.6 ± 4.1		43.5 ± 4.1	
β-amylase	49.8 ± 5.1		28.2 ± 4.6	
glucosidase	68.8 ± 2.5	25.4 ± 1.5	53.8 ± 2.5	18.1 ± 1.4

hollow capsules was caused by excess osmotic pressure of an outer PSS solution. The percentage of deformed microcapsule was an indication of the mechanical stability of microcapsules.[38,39] As shown in Figure 4, nearly 90% PSi microcapsules and ca.72% PTi microcapsules were broken after removing $CaCO_3$ template, and no intact PSi microcapsules and PTi microcapsules were observed in 16%(w/v) and 24%(w/v) PSS solution. But for PDA microcapsule, a deformation could be clearly observed. At 24%(w/v) PSS solution, 89% of PDA microcapsules, except broken microcapsules, were invaginated. However, only ~10% and ~3% of PSi-PDA and PTi-PDA microcapsules were shrunk in 40%(w/v) PSS solution. Obviously, the mechanical stability of the microcapsules was significantly improved by the synergistic effect between organic layer and inorganic layer. Additionally, because of the unique Ti(IV)-catechol interaction, PTi-PDA microcapsules showed much higher mechanical stability than PSi-PDA microcapsules.

The microcosmic configuration of PTi-PDA and PSi-PDA microcapsules was also investigated by HRSEM. As shown in Figure 5a and b, PTi-PDA microcapsule wall was of two-layered structure, while PSi-PDA microcapsule wall was of single-layered structure. The diameter of polydopamine particle ~100 nm in the PTi-PDA microcapsule was much larger than that of titania particle in the PTi microcapsule (20−40 nm) (Figure 5c).[16] There exist multiple interactions between the inorganic layer and the organic layer, such as hydrogen bond, ionic bond, and covalent bond. When a dopamine molecule adsorbs on titania, both terminal OH groups dissociate and the Hs bind to the O atoms to form additional surface hydroxyls (hydrogen bond).[40] Dopamine forms bidentate binuclear surface complexes on TiO_2 particles (each OH group from the dopamine binds to a separate Ti molecule on the exposed surface) in solution that appear to have a 40% covalent and 60% ionic bond characteristic.[41] Dopamine and Ti molecule formed complexes instantly, meanwhile, the self-polymerization of dopamine happened on the surface of PTi-PDA microcapsules. However, the diameter of polydopamine particle ca.20−30 nm in the PSi-PDA microcapsule (Figure 5d) was close to that of silica particle in the PSi microcapsule (20−25 nm).[42] Additionally, the XPS analysis indicated that only trace amount of Si element was remained on the outer surface of PSi-PDA microcapsule. Thus, it can be tentatively concluded that dopamine was self-polymerized on the surface of silica and formed a PSi-PDA particle. The adhesion of polydopamine to silica was much weaker and probably not due to a specific coordination complex as it was with titania, and instead, the Si-dopamine interaction might be ascribed to hydrogen bonding between the OH groups of the catechol and the O atom in silica.[43]

To explore the application potential of the hybrid microcapsules, a multienzyme system containing three enzymes was constructed for converting starch to isomaltooligosaccharide (IMOs). α-amylase, β-amylase, and glucosidase were respectively immobilized through physical encapsulation in the lumen,[44,45] in situ

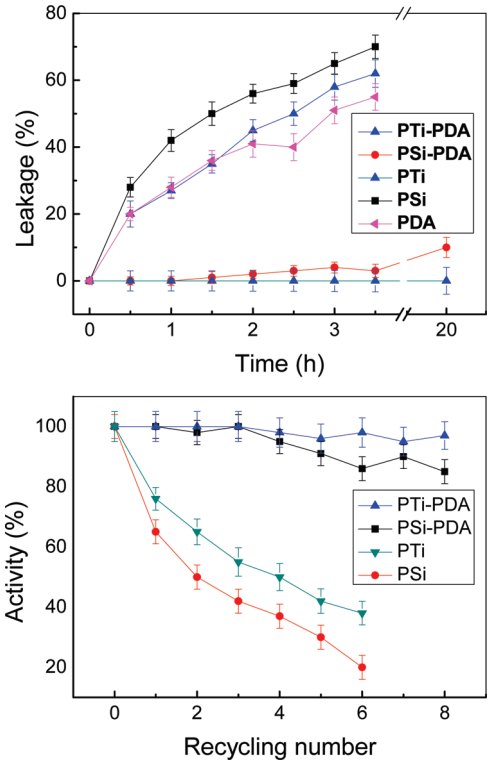

Figure 6. (a) Leakage of the micromicrocapsules. (b) Recycling stability of the multienzyme system.

entrapment within the wall[46] and chemical attachment on the out surface of the hybrid microcapsules.[27] The immobilization yields of α-amylase, β-amylase and glucosidase were summarized in Table 1. The immobilization yield of α-amylase was similar in PSi-PDA and PTi-PDA microcapsules due to the same surface property of the two kinds of microcapsules. The immobilization yield of β-amylase in PTi-PDA microcapsule was higher than that in PSi-PDA microcapsule because of the thicker polydopamine layer in PTi-PDA microcapsule. The immobilization yield of glucosidase in PTi-PDA microcapsules was higher than that in PSi-PDA microcapsules due to higher mechanical stability of PTi-PDA microcapsules. The leakage of glucosidase encapsulated in PSi-PDA, PSi, PTi-PDA, PTi, and PDA was shown in Figure 6a. About 70%, 65%, and 55% of glucosidase was leaked from the PSi, PTi, and PDA microcapsules within 3.5 h, respectively. In sharp contrast, only 10% of glucosidase was leaked from PSi-PDA microcapsules after 20 h, and no glucosidase leakage from PTi-PDA microcapsules was detected after 20 h. The isomaltooligosaccharides(IMOs), oligosaccharides with an a-D-$^{1-6}$ linkage including isomaltose, panose and isomaltotriose, were produced from corn starch by sequential reactions of starch with α-amylase, β-amylase and glucosidase, which was enabled by the multienzyme system. Figure 6b illustrated the recycling stability of the multienzyme system immobilized by PSi-PDA and PTi-PDA microcapsule. After eight repeated batches, the overall catalytic activity of the immobilized multienzyme system only reduced 15% in PSi-PDA microcapsule and quite surprisingly, almost no catalytic activity loss could be found for PTi-PDA microcapsule, indicating the excellent recycling behavior arising from the appropriate microenvironment including the biocompatibility, mechanical, and structural stability of these hybrid microcapsules.

4. CONCLUSIONS

In this study, a novel and facile biospired approach was developed to prepared organic−inorganic hybrid microcapsule via the combination of biomimetic mineralization and bioadhesion under mild conditions. Because of the coordination interaction between the titanium ions in the biomineral layer and catechol groups in the bioadhesive layer, the hybrid microcapsules displayed significantly improved mechanical stability; moreover, the polydopamine-coated microcapsule surface rendered the reactive platform for secondary treatments. Both the structures (thickness, porosity, etc.) of the biomineral layer and the bioadhesive layer could be flexibly tuned by varying the concentration of inorganic precursor/dopamine, temperature and pH values of aqueous solution. The interfacial binding strength between the biomineral layer and the bioadhesive layer could be tuned by varying the type of inorganic precursor and bioadhesive. Hopefully, the reported approach could be extended to prepare virtually any forms of organic−inorganic hybrid materials (films, tubules etc.). In particular, this study would be helpful for understanding the hierarchical structure evolution of some biological systems. Moreover, the hybrid microcapsules were readily utilized for constructing multienzyme system, in which three enzymes are respectively immobilized through physical encapsulation in the lumen, in situ entrapment within the wall and chemical attachment on the out surface of the hybrid microcapsules. The as-constructed multienzyme system displays desired catalytic activity and high recycling stability. Besides biocatalysis, the hybrid microcapsules can be expected to be highly applicable in biomedical and biosensing fields.

■ ASSOCIATED CONTENT

Supporting Information. Additional material as described in the text. This material is available free of charge via the Internet at http://pubs.acs.org.

■ AUTHOR INFORMATION

Corresponding Author
*E-mail: zhyjiang@tju.edu.cn.

■ ACKNOWLEDGMENT

The authors appreciate the financial support from the National Basic Research Program of China (2009CB724705), the National Science Foundation (20976127), the Programme of Introducing Talents of Discipline to Universities (No. B06006), and the program for Changjiang Scholars and Innovative Research Team in University (PCSIRT).

■ REFERENCES

(1) Sumper, M.; Brunner, E. *Adv. Funct. Mater.* **2006**, *16*, 17–26.
(2) Aizenberg, J.; Weaver, J. C.; Thanawala, M. S.; Sundar, V. C.; Morse, D. E.; Fratzl, P. *Science* **2005**, *309*, 275–278.
(3) Addadi, L.; Joester, D.; Nudelman, F.; Weiner, S. *Chem.—Eur. J.* **2006**, *12*, 980–987.
(4) Fakhrullin, R.; Minullina, R. *Langmuir* **2009**, *25*, 6617–6621.
(5) Holt, B.; Lam, R.; Meldrum, F. C.; Stoyanov, S. D.; Paunov, V. N. *Soft Matter* **2007**, *3*, 188–190.
(6) Fakhrullin, R.; Paunov, V. *Chem. Commun.* **2009**, *2009*, 2511–2513.
(7) Jan, J. S.; Shantz, D. *Adv. Mater.* **2007**, *19*, 2951–2956.
(8) Sollner, C.; Burghammer, M.; Busch-Nentwich, E.; Berger, J.; Schwarz, H.; Riekel, C.; Nicolson, T. *Science* **2003**, *302*, 282–286.
(9) Khan, F.; Walsh, D.; Patil, A. J.; Perriman, A. W.; Mann, S. *Soft Matter* **2009**, *5*, 3081–3085.
(10) Coradin, T.; Mercey, E.; Lisnard, L.; Livage, J. *Chem. Commun.* **2001**, 2496–2497.
(11) Luckarift, H.; Spain, J.; Naik, R.; Stone, M. *Nat. Biotechnol.* **2004**, *22*, 211–213.
(12) Pouget, E.; Dujardin, E.; Cavalier, A.; Moreac, A.; Valery, C.; Marchi-Artzner, V.; Weiss, T.; Renault, A.; Paternostre, M.; Artzner, F. *Nat. Mater.* **2007**, *6*, 434–439.
(13) Sanchez, C.; Arribart, H.; Giraud Guille, M. M. *Nat. Mater.* **2005**, *4*, 277–288.
(14) Jiang, Y.; Yang, D.; Zhang, L.; Sun, Q.; Zhang, Y.; Li, J.; Jiang, Z. *Dalton Trans.* **2008**, 4165–4171.
(15) Li, L.; Jiang, Z.; Wu, H.; Feng, Y.; Li, J. *Mater. Sci. Eng. C* **2009**, *29*, 2029–2035.
(16) Jiang, Y.; Yang, D.; Zhang, L.; Sun, Q.; Sun, X.; Li, J.; Jiang, Z. *Adv. Funct. Mater.* **2009**, *19*, 150–156.
(17) Li, J.; Jiang, Z.; Wu, H.; Zhang, L.; Long, L.; Jiang, Y. *Soft Matter* **2010**, *6*, 542–550.
(18) Lee, H.; Scherer, N.; Messersmith, P. *Proc. Natl. Acad. Sci.* **2006**, *103*, 12999–13003.
(19) Sever, M. J.; Weisser, J. T.; Monahan, J.; Srinivasan, S.; Wilker, J. J. *Angew. Chem., Int. Ed.* **2004**, *43*, 448–450.
(20) Lin, Q.; Gourdon, D.; Sun, C.; Holten-Andersen, N.; Anderson, T.; Waite, J.; Israelachvili, J. *Proc. Natl. Acad. Sci.* **2007**, *104*, 3782–3876.
(21) Wilker, J. *Angew. Chem., Int. Ed.* **2010**, *49*, 8076–8078.
(22) Harrington, M. J.; Masic, A.; Holten-Andersen, N.; Waite, J. H.; Fratzl, P. *Science* **2010**, *328*, 216–220.
(23) Wilker, J. *Curr. Opin. Chem. Biol.* **2010**, *14*, 276–283.
(24) Messersmith, P. B. *Science* **2008**, *319*, 1767–1768.
(25) Postma, A.; Yan, Y.; Wang, Y.; Zelikin, A. N.; Tjipto, E.; Caruso, F. *Chem. Mater.* **2009**, *21*, 3042–3044.
(26) Waite, J. *Nat. Mater.* **2008**, *7*, 8–9.
(27) Lee, H.; Rho, J.; Messersmith, P. *Adv. Mater.* **2009**, *21*, 431–434.
(28) Wang, Y.; Hang, K.; Anderson, N. A.; Lian, T. *J. Phys. Chem. B* **2003**, *107*, 9434–9440.
(29) Creutz, C.; Chou, M. H. *Inorg. Chem.* **2008**, *47*, 3509–3514.
(30) Petrov, A. I.; Volodkin, D. V.; Sukhorukov, G. B. *Biotechnol. Prog.* **2005**, *21*, 918–925.
(31) Tong, W.; Dong, W.; Gao, C.; Möhwald, H. *J. Phys. Chem. B* **2005**, *109*, 13159–13165.
(32) Fujiwara, M.; Shiokawa, K.; Araki, M.; Ashitaka, N.; Morigaki, K.; Kubota, T.; Nakahara, Y. *Cryst. Growth Des.* **2010**, *10*, 4030–4037.
(33) Zhang, L.; Jiang, Y.; Jiang, Z.; Sun, X.; Shi, J.; Cheng, W.; Sun, Q. *Biochem. Eng. J.* **2009**, *46*, 186–192.
(34) Tong, W.; Song, H.; Gao, C.; Möhwald, H. *J. Phys. Chem. B* **2006**, *110*, 12905–12909.
(35) Moser, J.; Punchihewa, S.; Infelta, P. P.; Graetzel, M. *Langmuir* **1991**, *7*, 3012–3018.
(36) Liu, Y.; Dadap, J. I.; Zimdars, D.; Eisenthal, K. B. *J. Phys. Chem. B* **1999**, *103*, 2480–2486.
(37) Ivnitski, D.; Artyushkova, K.; Rincón, R.; Atanassov, P.; Luckarift, H.; Johnson, G. *Small* **2008**, *4*, 357–364.
(38) Vinogradova, O.; Lebedeva, O.; Kim, B. *Mater. Res.* **2006**, *36*, 143–178.
(39) Fery, A.; Weinkamer, R. *Polymer* **2007**, *48*, 7221–7235.
(40) Li, S.-C.; Chu, L.-N.; Gong, X.-Q.; Diebold, U. *Science* **2010**, *328*, 882–884.
(41) Martin, S. T.; Kesselman, J. M.; Park, D. S.; Lewis, N. S.; Hoffmann, M. R. *Environ. Sci. Technol.* **1996**, *30*, 2535–2542.
(42) Zhang, Y.; Wu, H.; Li, J.; Li, L.; Jiang, Y.; Jiang, Y.; Jiang, Z. *Chem. Mater.* **2007**, *20*, 1041–1048.
(43) Anderson, T. H.; Yu, J.; Estrada, A.; Hammer, M. U.; Waite, J. H.; Israelachvili, J. N. *Adv. Funct. Mater.* **2010**, *20*, 4196–4205.

(44) Cui, J.; Wang, Y.; Postma, A.; Hao, J.; Hosta-Rigau, L.; Caruso, F. *Adv. Funct. Mater.* **2010**, *20*, 1625–1631.
(45) Fu, Y.; Li, P.; Xie, Q.; Xu, X.; Lei, L.; Chen, C.; Zou, C.; Deng, W.; Yao, S. *Adv. Funct. Mater.* **2009**, *19*, 1784–1791.
(46) Zhou, W.; Lu, C.; Guo, X.; Chen, F.; Yang, H.; Wang, X. *J. Mater. Chem.* **2010**, *20*, 880–883.